Journal of The Electrochemical Society, **154** (4) A343-A346 (2007)
0013-4651/2007/154(4)/A343/4/$20.00 © The Electrochemical Society

Synthesis and Optimization of Nanoparticle Ge Confined in a Carbon Matrix for Lithium Battery Anode Material

Hyojin Lee,[a] Hansu Kim,[b] Seok-Gwang Doo,[b] and Jaephil Cho[a,*,z]

[a]*Department of Applied Chemistry, Kumoh National Institute of Technology, Gumi, Korea*
[b]*Materials Research Center, Samsung Advanced Institute of Technology, Giheung, Yongin, Korea*

Ge nanoparticles with different particle sizes confined in a carbon matrix were prepared by annealing Ge nanoparticles terminated with butyl groups at 400, 600, and 800°C. X-ray diffraction and transmission electron microscopy results showed that the Ge nanoparticles' size increased from 8 to 100 nm as the annealing temperature of the as-prepared samples increased from 400 to 800°C. Raman spectra confirmed that the parts of the Ge nanoparticles were not covered by the carbon starting at 600°C after annealing for 9 h. Moreover, the graphitization degree of the carbon increases with increasing temperature, and the sample, annealed at 800°C for 3 h, showed the graphitization degree. Electrochemical cycling results revealed that the 10 nm Ge nanoparticles, confined in a carbon matrix obtained after annealing the as-prepared sample at 600°C for 3 h, showed the best charge capacity of 1067 mAh/g with 12% capacity loss after 30 cycles. On the other hand, Ge nanoparticles that had not been covered with the carbon matrix showed a rapid capacity decrease, along with pulverization of Ge nanoparticles to a size of about 5–10 nm after cycling.
 [DOI: 10.1149/1.2437059]

Manuscript submitted September 28, 2006; revised manuscript received December 5, 2006.
Available electronically February 21, 2007.

Group III, IV, V elements are commonly investigated as anode materials in lithium secondary batteries with Si, Ge, and Sn being the most popular and interesting materials.[1-5] Si and Ge showed specific capacities of 4000 and 1600 mAh/g, respectively, when forming the $Li_{21}M_5$ alloy.[6-10] Despite these capacities, these materials exhibited a rapid capacity loss, accompanied by huge irreversible capacity, with the bulk metals approaching nearly 0 mAh/g after several cycles. In these studies, the materials have been acquired from sputtering and ballmilling. Considering practical aspects for using these materials in Li secondary batteries, particles are a more appropriate choice than thin films, and uniformly sized nanoparticles should be used for reducing inhomogeneous volume expansion between the particles.

There has been much interest in Si and Ge nanocrystals, especially in regards to the potential of obtaining useful levels of visible photoluminescence (PL) from these materials,[11] So far, Ge nanocrystals have been produced by a variety of techniques, including sputtering,[12] laser ablation,[13] sol-gel processing,[14] and ion implantation followed by high-temperature annealing.[15] However, these techniques produce broad distributions of crystal sizes, along with broad optical absorption and PL features that make definitive interpretation in terms of quantum confinement difficult.[13] It has been reported that solution-based synthesis of nanocrystals of these materials is more difficult than for the compound semiconductors. This factor has been largely responsible for the lack of highly crystalline monodisperse samples. Controlled nucleation and growth occur in the interior of nanosize surfactant aggregates, called inverse micelles.[14] An anhydrous ionic salt, such as GeX_4 (X = Cl,Br), is dissolved in the hydrophilic interior of a solution of micelles. Since the ionic salts are completely insoluble in the continuous oil medium used, the nucleation and growth of Ge is restricted to the micelle interior. However, this method should use a reducing agent, such as $LiAlH_4$, to reduce Ge(IV) to Ge(0) in water. In addition, there is a possibility of competing hydrolysis to GeO_2 because of the presence of water.

There have been reports of the low-temperature solution synthesis of Si and Ge nanoclusters terminated by alkyl groups. This synthesis utilizes reactive Zintl salts (KGe and NaGe). For instance, Taylor et al.[16] reported that the metathesis reaction of NaGe with excess $GeCl_4$ in glyme solvents produced Ge nanocrystals. However, there was no measured particle size distribution for these nanocrystals obtained without further annealing. The X-ray diffraction (XRD) patterns of the further annealed sample at 600°C, on the other hand, showed a mean particle size smaller than 10 nm.

In this study, we report the synthesis and optimization of Ge nanoparticle size confined in the carbon matrix for use as anode materials in lithium secondary batteries, and Ge nanoparticle size ranged between 10 and 100 nm, depending on an annealing temperature.

Experimental

For synthesizing the butyl-capped Ge nanoparticles, all the experimental procedures were carried out in inert atmosphere except for the washing process. Sodium naphthalide solution was prepared from 5.4 g (0.23 mole) of sodium and 19.38 g (0.15 mole) of naphthalene, stirred in 100 mL 1.2-dimethoxyethane; 4.56 mL (0.022 mol) of $GeCl_4$ and 100 mL of 1.2-dimethoxyethane solvent were thoroughly mixed and decanted into the sodium naphthalide solution. This mixed solution was stirred for 2 h, and then 60 mL of butyllithium was added. Instantly, the solution turned orange, and the solvent and naphthalene were removed by using a rotating evaporator at 90°C for 6 h. After the washing process, a viscous orange oil was obtained, and it was washed six times with water. The orange oil was annealed at 400, 600, and 800°C for 3 h and 600°C for 9 h in a vacuum furnace to obtain a dark brown powder.

The cathodes for the battery test cells were made of butyl-capped Ge material, super P carbon black, and polyvinylidene fluoride (PVDF) binder (Solef) in a weight ratio of 8:1:1. The slurry was prepared by thoroughly mixing a *N*-methyl-2-pyrrolidone (Aldrich) solution of PVDF, carbon black, and the anode material. The coin-type half cells (2016R size), prepared in a helium-filled glovebox, contained a cathode, a Li metal anode, a microporous polyethylene separator, and an electrolyte solution of 1 M $LiPF_6$ in ethylene carbonate/dimethyl carbonate (1:1 vol %) (Cheil Industries).

A field-emission transition electron microscopy (TEM) (JEOL 2100F), operating at 200 kV, was used for investigating the microstructure of the samples. Raman spectroscopy (Renishaw 3000) was used to characterize Ge nanocrystals confined in an amorphous carbon matrix and to obtain the graphitization degree of an amorphous carbon phase in the sample (ratio of *D* and *G* band of the carbon), using 633 nm laser excitation. Fourier transform infrared (FTIR) spectra (JASCO 4000) for the nanoparticles were obtained at room temperature by dropping the hexane colloid on a KBr plate and allowing the solvent to evaporate.

* Electrochemical Society Active Member.
z E-mail: jpcho@kumoh.ac.kr

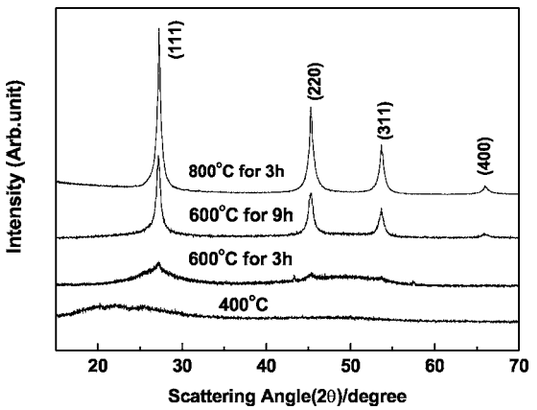

Figure 1. XRD patterns of the samples before and after annealing at 400°C for 3 h, 600°C for 3 and 9 h, and 800°C for 3 h.

Results and Discussion

Figure 1 shows the XRD patterns of the samples before and after annealing at 400, 600, and 800°C for different times. The XRD pattern of the as-prepared sample confirmed the presence of amorphous Ge particles. As the annealing temperature increased, the XRD patterns started to sharpen and peaks were clearly distinguishable. The size of the annealed Ge nanoparticles was determined from the width of the peaks according to the Debye-Scherr equation,[17] and the annealed samples at 600°C for 3 and 9 h were estimated to be 8 and 15 nm, respectively. When the sample was annealed at 800°C for 3 h, the particle size increased to 100 nm. Figure 2 shows Raman spectra of the samples annealed at 400°C for 3 h, 600°C for 3 and 9 h, and 800°C for 3 h. Except for the sample annealed at 400°C, the spectra of the other samples show the carbon peaks at 1360 and 1580 cm^{-1}, corresponding to D and G bands, respectively. D/G ratio in the Raman spectra was determined by integrating each area of the bands. The D/G ratio, indicative of the graphitization degree of carbon, of the samples decreased with increasing annealing temperature and time at 600°C for 3 or 9 h and 800°C for 3 h, with the values of 2.5, 2.0, and 1.5, respectively. For comparison, the D/G ratio for synthetic graphite was less than 0.09.[18] This indicates that the sample annealed at 800°C has the highest graphitization degree among the samples. Amorphous carbon has limited Li intercalation/deintercalation amounts, depending on the graphitization degree, and its lower graphitization degree

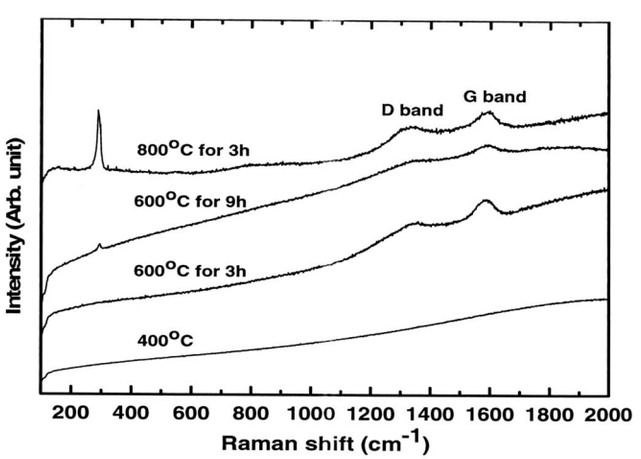

Figure 2. Raman spectra of the samples annealed at 400°C for 3 h, 600°C for 3 and 9 h, and 800°C for 3 h.

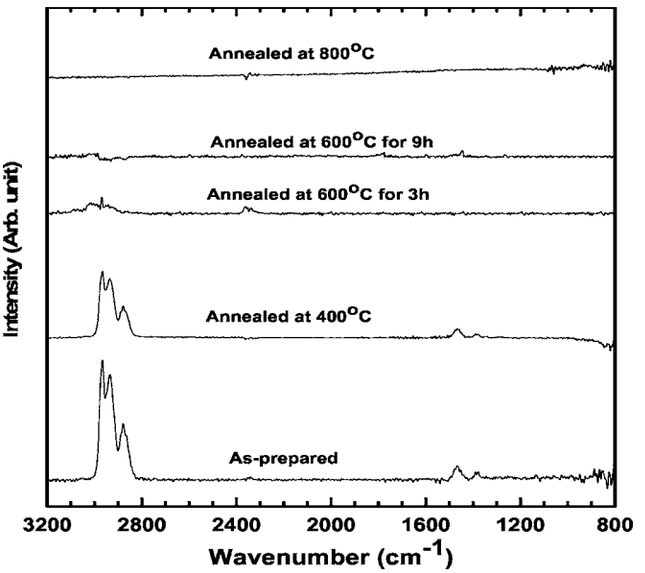

Figure 3. FTIR spectra of the samples before and after annealing at 400°C for 3 h, 600°C for 3 and 9 h, and 800°C for 3 h.

leads to lower capacity.[18] In addition, it should be noted that the samples annealed at 600 and 800°C for 9 and 3 h showed the Ge–Ge vibration band at 287 cm^{-1}, and its intensity increased with increasing annealing temperature, indicating that Ge nanoparticles were not completely covered with a carbon layer. The combined XRD and Raman spectral results indicate that 8 nm Ge nanoparticles were surrounded by the carbon. However, the sample annealed at 800°C showed a large portion of the Ge nanoparticles was not covered by the carbon. Therefore, Ge nanoparticles are expected to agglomerate into larger particles at higher annealing temperatures.

Figure 3 shows FTIR spectra of the butyl-capped Ge particles before and after annealing at 400, 600, and 800°C. The three peaks at 2955, 2924, and 2853 cm^{-1} fall where expected for C–H stretches of butyl groups which was well matched with the result in Ref. 16 The peaks at 1376 and 1456 cm^{-1} are the positions expected for the symmetric and asymmetric bends of the butyl group, respectively. As can be seen in Fig. 3, as the annealing temperature increased, the peak intensities assigned to butyl groups rapidly decreased, and the samples annealed at 600°C for 9 h and 800°C for 3 h showed no traces of the butyl groups, indicating complete transformation into amorphous carbon. In the case of the sample annealed at 600°C for 3 h, small residual C_4H_9 peaks were observed.

In order to support these spectra results, TEM analysis (Fig. 4a-f) was performed, using the samples before and after annealing. The as-prepared sample shows a particle size distribution between 1 and 0.5 μm, but, after annealing at 400°C, 8 nm Ge nanoparticles were confined to a different phase, which is believed to be carbon. This result reveals that the as-prepared sample consisted of micrometer-sized particles which contained many 8 nm Ge particles capped with butyl groups, as shown in Fig. 5. In the case of the sample annealed at 600°C for 3 h (Fig. 4c and d), no apparent Ge particle growth was observed showing the same particle size as above. The expanded TEM image of Fig. 4c clearly shows the {220} lattice fringe of the Ge (Fig. 4d). Upon extending the annealing time to 9 h, nonuniformly distributed Ge nanoparticles were observed with particle sizes ranging from 10 to 20 nm (Fig. 4e). This is due to Ge nanoparticles that were not capped with carbon layers which would have aggregated to create larger particle sizes. A similar result was also observed in the sample annealed at 800°C, with severely aggregated Ge particles having a particle size of about 100 nm, which was 12 times larger than the one annealed at 600°C for 3 h. Such a large particle size is believed to be induced by accelerated disappearance

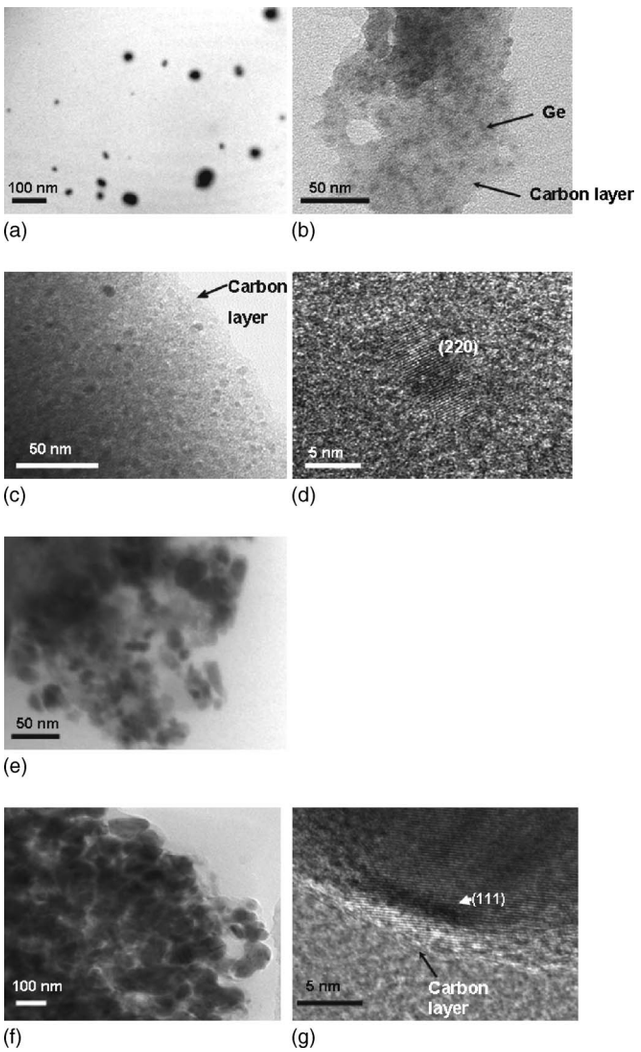

Figure 4. TEM images of the samples (a) before and after annealing at (b) 400°C for 3 h, 600°C for (c) 3 h and (e) 9 h, and 800°C for (f) 3 h. Parts (d) and (g) are expanded TEM images of (c) and (f), respectively.

of the capped carbon layer on the particle, which acts as an inhibitor for interparticle conglomeration. In this case, we clearly observed {111}, a lattice fringe, along with a carbon layer of ~1 nm. Table I exhibits the composition of the samples measured by CHS and inductively coupled plasma (ICP) analysis. H content rapidly decreases with increasing annealing temperature, and the sample annealed at 800°C has negligible amount of hydrogen.

Electrochemical testing was performed, using the annealed samples at different temperatures in coin-type half cells, at a rate of

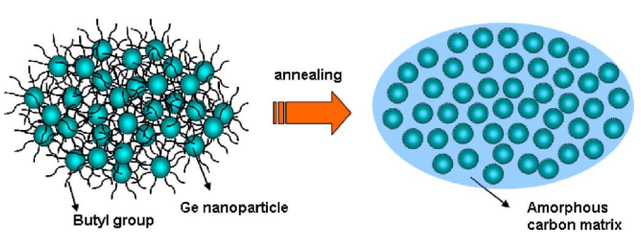

Figure 5. (Color online) Schematic view showing the formation of Ge nanoparticles confined in an amorphous carbon matrix after annealing.

Table I. The compositions of the samples measured by ICP and CHS analyzers.

	H (wt %)	C (wt %)	Ge (wt %)
400°C	9	11.5	79.5
600°C for 3 h	1.1	10.5	88.4
600°C for 9 h	0.1	9.6	90.3
800°C for 3 h	0	6.8	93.2

0.2 C (1C = 1600 mA/g) between 0 and 1.2 V, as shown in Fig. 6. Ge nanoparticles obtained from annealing at 400°C for 3 h showed a small charge capacity of 312 mAh/g, with an irreversible capacity ratio of 69%, which was due to the low graphitization degree of the carbon. However, the sample annealed at 600°C for 3 h showed a significantly improved charge capacity of 1067 mAh/g, with an irreversible capacity ratio of 26% and capacity retention after 30 cycles of 88% (voltage profiles the sample annealed at 600°C for 3 h after 2, 10, 20, and 30 cycles were shown in Fig. 7). The electrode density of the Ge embedded in a carbon matrix after discharging to 0 V was 1.5 g/cm^3 (due to the volume expansion of the electrode after lithium alloying, it is reasonable to estimate the electrode density using discharged electrode). The case of the sample annealed at 600°C for 9 h had a first charge capacity of 975 mAh/g, and, compared to the sample annealed at 600°C for 3 h, had an increased irreversible capacity ratio of 42%. This was due to enhanced side reactions with the electrolytes of the uncovered parts with the carbon layer. In addition, note that capacity retention was decreased by 27%, compared with the sample annealed at 600°C for 3 h. These results suggest that the increased graphitization degree of the carbon and carbon matrix improved the capacity of the Ge nanoparticles. In the case of the sample annealed at 800°C, its charge capacity was 1748 mAh/g, with an irreversible capacity ratio of 24%, which was the smallest value among the samples. This is

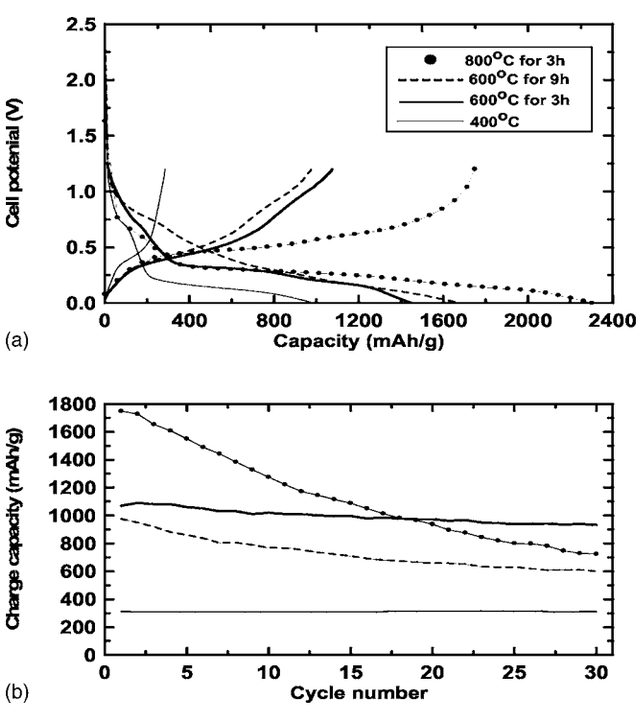

Figure 6. (a) Voltage profiles of the samples annealed at 400°C for 3 h, 600°C for 3 h, 9 h, and 800°C for 3 h in coin type half cells at a rate of 0.2°C between 0 and 1.2 V during the first cycle. (b) Cycle number vs charge capacity of (a).

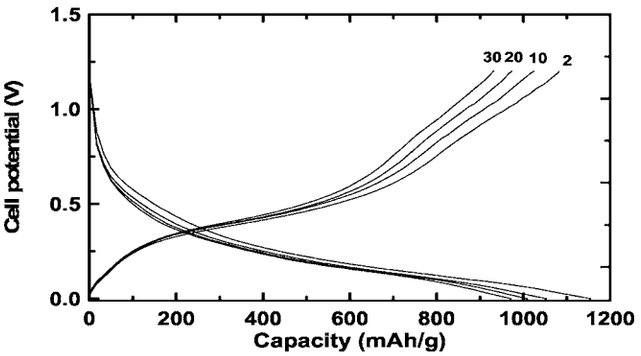

Figure 7. Voltage profiles for the sample annealed at 600°C for 3 h after 2, 10, 20, and 30 cycles at the same test condition to Fig. 6.

believed to be due to enhanced graphitization degree of the carbon layer. However, its capacity decreased to 729 mAh/g after 30 cycles corresponding to a capacity retention value of 42%. Considering capacity contribution of the amorphous carbon (amorphous carbon showed the reversible capacity of ~100 mAh/g),[2] its effect on the total capacity of the samples is negligible.

Using the cycled electrodes, the particle size and morphology were analyzed. The sample annealed at 600°C for 3 h showed a particle size identical to that before cycling (Fig. 8a). Further, Ge nanoparticles were well dispersed without showing aggregation. On the other hand, a cycled electrode, obtained from annealing at 600°C for 9 h, showed an increased particle size to 20–30 nm, compared to that before cycling (Fig. 8b). In addition, partial particle aggregation with different lattice fringes (Fig. 8c) is observed, indicating that some particle breakup and subsequent aggregation occurred. Finally, rapid capacity fading of the sample annealed at 800°C was due to severe particle pulverization and direct electric disconnection from the current collector. The TEM image of the cycled sample in Fig. 8d shows direct evidence for this, with a particle size of about 10 nm. That is, the original 100 nm Ge nanoparticles were pulverized to 10 nm ones. Similar behavior was observed in mesoporous tin phosphate anode material with a cellular foam structure.

Conclusions

Ge nanoparticles, surrounded by carbon, showed the best electrochemical performance when the butyl-capped Ge nanoparticles were annealed at 600°C for 3 h. The first charge capacity was 1067 mAh/g, with an 88% capacity retention after 30 cycles. We believe that this effect was associated with the carbon layer, which acted as a buffer layer for volume expansion of the Ge nanoparticles. More importantly, uniformly formed Ge nanocrystals provided very little volume expansion between Ge and Li_xGe during Li alloying/dealloying.

Acknowledgment

This work was supported by the Korea Research Fondation Grant funded by the Korean Government (MOEHRD, Basic Research Promotion Fund) (KRF-2006-003-C00162).

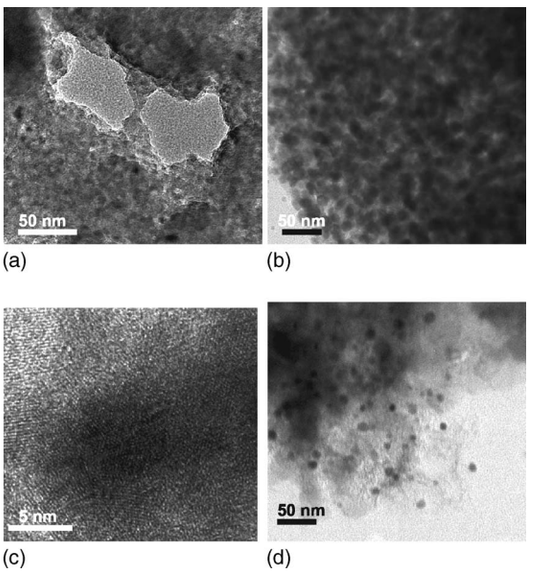

Figure 8. TEM images of the samples after annealing at 600°C for (a) 3 h and (b and c) 9 h, and (d) 800°C for 3 h after cycling; (c) is an expanded TEM image of (b).

Kumoh National Institute of Technology assisted in meeting the publication costs of this article.

References

1. J. O. Besenhard, J. Yang, and M. Winter, *J. Power Sources*, **68**, 87 (1997).
2. M. Noh, Y. Kwon, H. Lee, J. Cho, Y. Kim, and M. G. Kim, *Chem. Mater.*, **17**, 1926 (2005).
3. M. Noh, Y. Kim, M. G. Kim, H. Lee, H. Kim, Y. Kwon, Y. Lee, and J. Cho, *Chem. Mater.*, **17**, 3320 (2005).
4. Y. Kwon, M. G. Kim, Y. Kim, Y. Lee, and J. Cho, *Electrochem. Solid-State Lett.*, **9**, A34 (2006).
5. S. Bourderau, T. D. Brousse, and M. Schleich, *J. Power Sources*, **81**, 233 (1999).
6. J. Graetz, C. C. Ahn, R. Yazami, and B. Fultz, *J. Electrochem. Soc.*, **151**, A698 (2004).
7. M. N. Obrovac and L. Christensen, *Electrochem. Solid-State Lett.*, **7**, A93 (2004).
8. W. J. Weydanz, M. Wohlfahrt-Mehrens, and R. A. Huggins, *J. Power Sources*, **81**, 237 (2003).
9. B. Gao, S. Sinha, L. Fleming, and O. Zhou, *Adv. Mater. (Weinheim, Ger.)*, **13**, 816 (2001).
10. H. Lee, M. G. Kim, C. H. Choi, Y.-K. Sun, C. S. Yoon, and J. Cho, *J. Phys. Chem. B*, **109**, 20719 (2005).
11. J. P. Wilcoxon, P. P. Provencio, and G. A. Samara, *Phys. Rev. B*, **64**, 035417 (2001).
12. S. Hayashi, M. Fujii, and K. Yamamoto, *Jpn. J. Appl. Phys., Part 2*, **28**, L1464 (1989).
13. Y. Maeda, N. Tsukamoto, Y. Yazawa, Y. Kanemitsu, and Y. Masumoto, *Appl. Phys. Lett.*, **59**, 3168 (1991).
14. M. Zacharias and P. M. Fauchert, *Appl. Phys. Lett.*, **71**, 380 (1997).
15. S.-T. Ngiam, K. F. Jensen, and K. D. Kolenbrander, *J. Appl. Phys.*, **76**, 8201 (1994).
16. B. R. Taylor, S. M. Kauzlarich, H. W. H. Lee, and G. R. Delgado, *Chem. Mater.*, **11**, 2493 (1999).
17. B. D. Cullity, *Elements of X-ray Diffraction*, 2nd ed., Addison-Wesley, Menlo Park, NJ (1978).
18. I. Mochida, C.-H. Ku, S.-H. Yoon, and Y. Korai, *J. Power Sources*, **75**, 214 (1998).